LETTERS
PUBLISHED ONLINE: 11 JULY 2010 | DOI: 10.1038/NMAT2796

nature materials

Aluminium at terapascal pressures

Chris J. Pickard[1]* and R. J. Needs[2]

Studying materials at terapascal (TPa) pressures will provide insights into the deep interiors of large planets and chemistry under extreme conditions[1,2]. The equation of state of aluminium is of interest because it is used as a standard material in shock-wave experiments and because it is a typical *sp*-bonded metal[1,3]. Here we use density-functional-theory methods and a random-searching approach to predict stable structures of aluminium at multiterapascal pressures, finding that the low-pressure close-packed structures transform to more open structures above 3.2 TPa (nearly ten times the pressure at the centre of the Earth), with an incommensurate host–guest structure being stable over a wide range of pressures and temperatures. We show that the high-pressure phases may be described by a two-component model consisting of positive ions and interstitial electron 'blobs', and propose that such structures are common in *sp*-bonded materials up to multiterapascal pressures.

Multiterapascal pressures occur in, for example, the deep interiors of massive planets, and they can be generated on the Earth's surface in technically challenging experiments. Aluminium (Al) has been compressed to 400 TPa under shock-wave conditions generated by an underground nuclear explosion[4,5], although such experiments cannot be carried out under present agreements. The development of powerful pulsed lasers and new methodologies for very high-pressure experiments has opened the way for studying materials at multiterapascal pressures. The National Ignition Facility at the Lawrence Livermore National Laboratory[6] is expected to achieve shockless quasi-isentropic compression above 2 TPa (ref. 2) and much higher pressures under shock-wave conditions. The equation of state (EoS) of a material, which gives the equilibrium relationship between the pressure, volume and temperature, is of fundamental importance in high-pressure science. Laser-induced shock-wave experiments use a plate made from a 'shock standard' material whose EoS must be well established, and metals such as aluminium, platinum and tungsten are often used[1,3]. Al is regarded as a typical *sp*-bonded metal, but its structures (and indeed those of all materials) are unknown at terapascal pressures.

Aluminium crystallizes in the face-centred-cubic (fcc) structure under ambient conditions. Powder X-ray diffraction experiments have revealed a phase transition to a hexagonal-close-packed (hcp) structure at 0.217 TPa (ref. 7). Density functional theory calculations have also predicted a transition to a body-centred-cubic (bcc) phase at about 0.38 TPa (ref. 8), although this has not yet been confirmed experimentally. No experimental or theoretical evidence for further solid–solid phase transitions has been reported. Developments in time-resolved X-ray diffraction methods are expected to enable the structures formed during high-pressure dynamical compressions to be glimpsed[2]. Determining crystal structures at terapascal pressures is, however, beyond the grasp of present experimental techniques, and theoretical predictions are the only viable option at the moment.

We have obtained candidate high-pressure structures using the *ab initio* random structure searching (AIRSS) approach[9], which has been successfully applied to a variety of systems[10–12]. In the basic AIRSS approach an ensemble of structures is created by generating unit cells of random shapes with reasonable volumes. The atoms are placed at random positions and the cell shapes and atomic positions relaxed to an enthalpy minimum at fixed pressure. In previous AIRSS studies[10,11,13], we used constraints to reduce the number of structural degrees of freedom, enabling us to study systems with over 100 atoms and several atomic species[13]. Here, however, we use unconstrained random searching, which gives excellent results for metallic elements in unit cells with up to roughly 20 atoms and increases the likelihood of finding unexpected structures.

The structure searches are described in the Methods section. We found particularly favourable structures with 11, 16 and 21 atoms, and we refer to the lowest enthalpy structures found in these cells as Al11, Al16 and Al21, respectively. These structures are periodic approximations to the incommensurate host–guest structure of phase IVa of barium (Ba; refs 14,15). Analogous structures have been reported in compressed strontium, scandium, arsenic, antimony and bismuth[15], although we are not aware of any previous suggestions of a stable host–guest structure in a group IIIB element such as Al. We also found higher-enthalpy host–guest structures, including one with 16 atoms that we shall refer to as Al16–*I4/mcm*. Host–guest structures often came up in our searches, accounting for 16% of the relaxed structures obtained in the 11-, 16- and 21-atom searches at 5 TPa. A body-centred-tetragonal (bct) phase becomes more stable than bcc at 5 TPa, but it is never the most stable (Fig. 1).

The most stable structure found in the pressure range 3.2–8.8 TPa was Al16 (Fig. 2), which shows the main features of the Ba-IVa structure. Each of the host–guest structures has the same host framework consisting of eight-atom units, but the number of guest atoms varies. For example, Al11 has three guest atoms for every eight host atoms, and we refer to it as an $x = 3$ structure, whereas Al16 corresponds to $x = 8/3$ and Al21 to $x = 5/2$. We also built a number of other host–guest structures 'by hand', following ref. 16, including one with $x = 2$ in a 40-atom cell, $x = 5/2$ with 42 atoms, $x = 11/4$ with 86 atoms, $x = 3$ with 22 atoms and $x = 7/2$ with 46 atoms. More details of these and other structures are given in the Supplementary Information.

A simple-hexagonal structure becomes the most stable phase at 8.8 TPa, but it undergoes a symmetry-lowering distortion to a structure of space group *Cmma* at around 10 TPa, see Supplementary Fig. S1. The most stable phases at 30 TPa are far from close packed. The natural unit of pressure for atomic systems can be taken to be (Rydberg Energy)/(Bohr radius^3)$\sim$15 TPa (ref. 17). At such pressures the work done by the applied pressure

[1]Department of Physics and Astronomy, University College London, Gower Street, London WC1E 6BT, UK, [2]Theory of Condensed Matter Group, Cavendish Laboratory, J J Thomson Avenue, Cambridge CB3 0HE, UK. *e-mail: c.pickard@ucl.ac.uk.

© 2010 Macmillan Publishers Limited. All rights reserved.

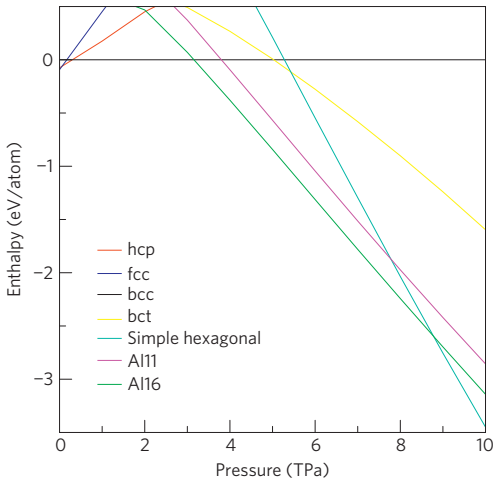

Figure 1 | Enthalpy–pressure relationships for Al phases. Enthalpy differences from the bcc phase are shown. The slopes of the curves give the volume differences from the bcc structure. The host–guest and simple hexagonal structures are favoured at high pressures because they are denser than the close-packed structures.

is comparable to the interaction energy of the valence electrons and ions, and it might be expected that materials would become close packed under such conditions[17]. Our study shows that this does not hold for Al, in which a rich structural physics persists to much higher pressures.

We have found good approximations to the Ba-IV incommensurate structure with remarkably few atoms. These structures reduce their enthalpies by symmetry-lowering distortions while retaining the essential features of the host–guest structure. The host–guest structures constructed by hand have higher symmetries and larger numbers of atoms. The equilibrium value of x at each pressure was obtained by fitting the enthalpies of the most stable structures to a quadratic curve; see Supplementary Fig. S2. The equilibrium value of x increases slowly with pressure and is well described within the range 3–8 TPa by $x = 2.543 + 0.0475p - 0.00259p^2$, where p is the pressure in TPa. This suggests that Al16 is a good approximation to the minimum-enthalpy structure around the predicted transition from bcc at 3.2 TPa and a somewhat poorer approximation at higher pressures.

We have calculated the vibrational modes of the bcc and Al16–*I4/mcm* (which is very similar in structure to, and slightly higher in enthalpy than, Al16) structures at several different pressures. The maximum phonon frequencies increase rapidly at low pressures, but they increase more slowly in the terapascal regime. For example, the highest vibrational frequencies of bcc are 2,170 cm^{-1} at 3 TPa and 2,510 cm^{-1} at 5 TPa, whereas the corresponding values for Al16–*I4/mcm* are 2,150 cm^{-1} at 3 TPa and 2,470 cm^{-1} at 5 TPa. The zero-point vibrational enthalpies have a negligible effect on the relative stabilities of the phases and the variation of volume with pressure over the range 1–10 TPa. The vibrational free energy of bcc at 10^4 K and 3 TPa is about 0.1 eV per atom lower than that of Al16–*I4/mcm*. The static lattice enthalpy of Al16–*I4/mcm* by 5 TPa is, however, about 0.9 eV per atom lower than that of bcc so that, even at 10^4 K, host–guest structures are by far the most stable. Liquid phases at multiterapascal pressures may also show large departures from close packing. We investigated the effects of electronic excitations at finite temperatures on the relative stability of the bcc and host–guest structures and found them to favour bcc by an additional 0.1 eV per atom at 10^4 K.

The predicted stability of the high-density host–guest and simple hexagonal structures significantly modifies the cold EoS shown in Fig. 3. Using the bcc phase would result in an overestimate of the volume by 2.8% at 5 TPa, where Al16 is stable, and by 5.6% at 10 TPa, where simple hexagonal is stable. The differences from published EoSs are also large. Our volume for Al16 at 5 TPa corresponds to a pressure of 5.4 TPa when using the EoS from refs 4,5 whereas our volume for simple hexagonal at 10 TPa corresponds to 11.5 TPa. The differences from the EoS of ref. 18 are even larger.

Solids are composed of almost incompressible ionic cores and more readily deformable valence-electronic charge density. Calculations at 5 TPa with the Al 1*s* core and 2*s* and 2*p* semicore orbitals described by a pseudopotential gave qualitatively similar results to the full calculations, demonstrating that deviations of these orbitals from their atomic forms are not important in stabilizing the high-pressure phases. Coulomb repulsion, Pauli exclusion and the orthogonality of orbitals pushes the 3*s*- and 3*p*-derived valence charge density away from the atomic nuclei[12,19], as shown in Supplementary Figs S5 and S6. This effect operates at all pressures, but the nearly-free-electron bandstructure of Al observed at ambient conditions is profoundly altered by the ionic cores at high pressures. The occupied valence bandwidths of the hcp, bcc and host–guest structures at 5 TPa are about half those obtained from the free-electron model at the same average densities. These deviations arise from the much larger fraction of the volume occupied by the cores at high pressures, which tends to localize valence electrons within interstitial pockets that are largely isolated from one another, narrowing the valence bands[12,19,20].

The main differences between the valence-electronic densities of states (e-DoS) of the bcc and host–guest structures at 5 TPa (see Supplementary Fig. S6) occur near the Fermi energy, with the more stable phases with lower e-DoS at the Fermi energy. This suggests that the relative stabilities of the bcc and host–guest phases are largely determined by the Fermi-surface mechanism invoked by Jones in 1934 to explain the distorted-cubic structure of bismuth[21,22]. Jones's idea was that the bandstructure energy can be lowered by the action of strong Fourier components of the lattice potential on the degenerate free-electron orbitals at the Bragg planes. If a Bragg plane grazes the surface of the occupied sphere of free-electron orbitals, the electronic energy levels just inside the Bragg plane are lowered in energy whereas those just outside are raised in energy, forming the valleys in the e-DoS near the Fermi energy visible in Supplementary Figs S5 and S6. This effect can lead to a substantial reduction in electronic energy, although it often increases the repulsive interaction between the ions. The effect of Jones's mechanism is amplified by the small occupied valence bandwidth. The e-DoS of simple-hexagonal structures (Supplementary Fig. S6) shows a substantial redistribution of valence electrons to lower energies compared with bcc and host–guest structures, whose occupied valence bandwidths are about 15% smaller. This effect is not connected with Jones's Fermi-surface mechanism; it arises instead from adopting a structure in which the valence electrons form interstitial layers, which widens the occupied valence band.

The structural phase transitions are accompanied by substantial changes in the charge density. At 5 TPa the maxima in the valence charge density of the bcc phase lie on intersecting lines whereas the host–guest structures exhibit distinct 'blobs' of valence charge density, as shown in Supplementary Fig. S3. The appearance of interstitial electron blobs has been described as the formation of an 'electride' in which the interstitial electrons are the anions[12,19,23,24]. The valence charge density of the higher-pressure simple hexagonal phase also shows interstitial blobs (Supplementary Fig. S4). Taking the peaks of the blobs as the anion positions and the Al ions as the cations, simple hexagonal Al is equivalent to the magnesium diboride (MgB_2) structure, with layers of Al ions separated by hexagonal-honeycomb layers of electrons.

We have studied the stability of host–guest structures in model systems described by a simple pairwise potential depending on the

© 2010 Macmillan Publishers Limited. All rights reserved.

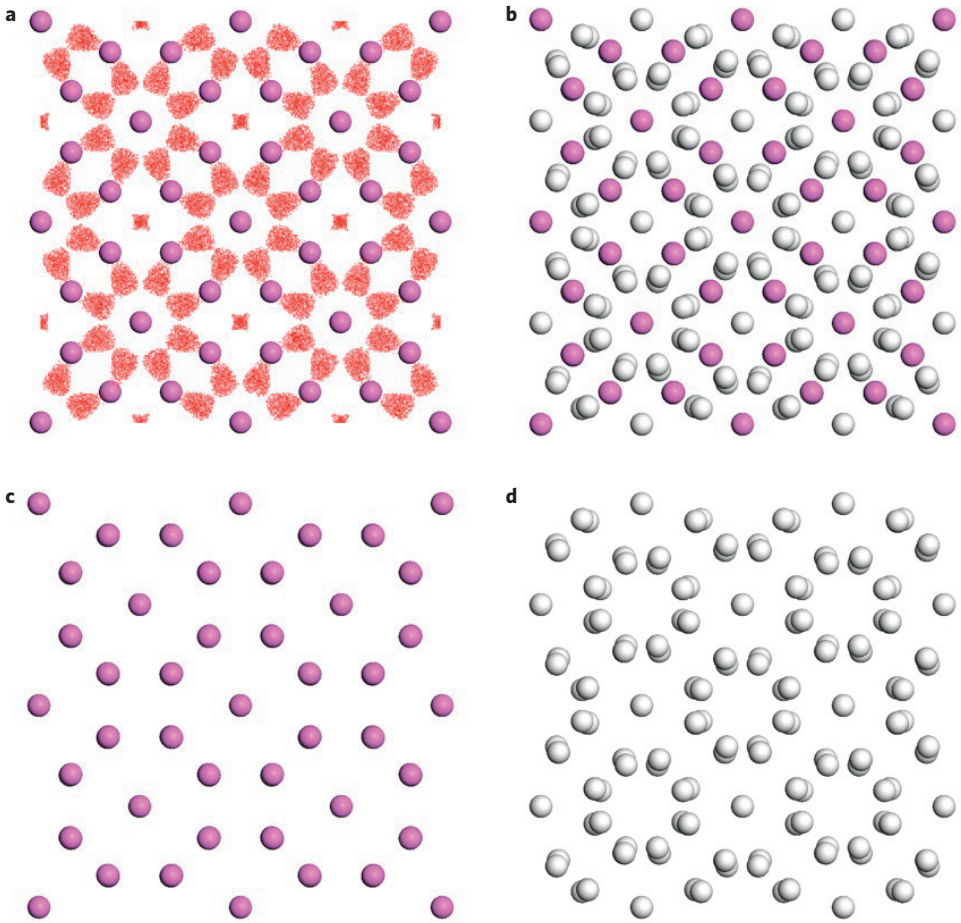

Figure 2 | Host-guest structures. a, The Al16 host-guest structure pictured along the axis of the guest chains, as obtained from density functional theory calculations. The guest atoms are at the centres of the octagonal rings. The red areas show the valence charge density above 65% of its maximum value. **b**, A structure obtained from random structure searching with simple pairwise potentials describing the interactions between 16 'Al' atoms (purple) and 28 'electron' blobs (white). **c**, The positions of the purple 'Al' ions from **b**, which gives a good approximation to the Ba-IV structure. **d**, The white 'electron' blobs from **b**, which give a good approximation to the Rb-IV structure.

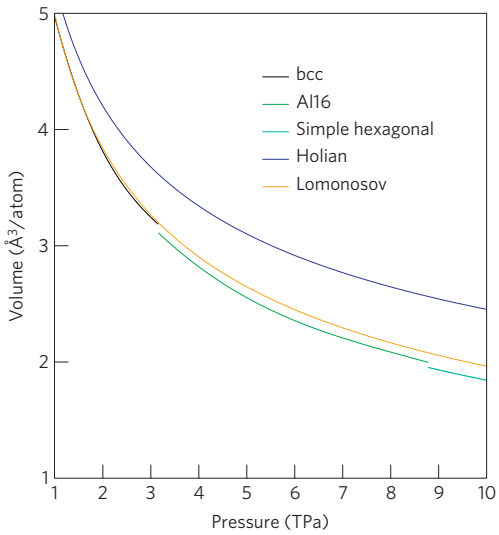

Figure 3 | Equation of state of Al. The volume–pressure relationship calculated in this work and from the EoSs of Lomonosov[4,5] and Holian[18].

distances between particles. The host–guest and simple hexagonal structures could only be generated using two species of particle, one describing the Al ions and the other describing the interstitial electron blobs. This suggests that the description of them as two-component electrides is appropriate. The Al16 host–guest structure has 12 host and four guest atoms, and by studying its charge density we deduced that it has two electron blobs per host atom and one per guest. We therefore carried out random structure searches with 16 'Al' atoms and 28 'electron' blobs, adjusting the potential to try to stabilize the Al16 phase. We readily found various potential parameters that stabilize the Al16 structure in some pressure range. These potentials generate a slightly distorted bcc phase as the most stable structure at lower pressures than Al16 and a slightly distorted sh phase at higher pressures, suggesting that they give a reasonable description of compressed Al and providing further support for the two-component hypothesis. The potentials have repulsive interactions between like species and attractive interactions between unlike, as expected for charged species. An example of such a potential is reported in the Supplementary Information.

Two elemental incommensurate host–guest structures are in fact known, the Ba-IV structure and the rubidium (Rb) IV structure found in the alkali metals Rb, potassium and sodium (Na) at high pressures[15,25]. We have discovered a remarkable duality between these structures. Consider the representation of a Ba-IV-like structure in terms of atoms and electron blobs. Although the atomic positions accurately approximate the Ba-IV incommensurate structure, the positions of the electron blobs accurately approximate the Rb-IV structure, as illustrated in Fig. 2.

© 2010 Macmillan Publishers Limited. All rights reserved.

The Ba-IV and Rb-IV structures are therefore related by reversing the roles of the ions and electron blobs. The ratio of blobs to ions is 7/4 in Al16 and very close to 4/7 for Na in the Rb-IV structure, consistent with the fact that Al has more valence electrons than Na and suggesting that the number of valence electrons is a crucial parameter in determining the nature of the electride structures.

We have also found other stable electride structures at terapascal pressures. We calculate that Mg transforms from fcc to simple hexagonal at ∼0.75 TPa, then to simple cubic at ∼1 TPa, and then to a structure of *Pnma* symmetry at ∼30 TPa. The simple hexagonal, simple cubic and *Pnma* structures are electrides, with simple hexagonal corresponding to the MgB_2 structure, simple cubic to the caesium chloride (CsCl) structure and *Pnma* to the iron boride (FeB) structure. We have also found that an electride structure of Na of *Pnma* symmetry with chains of interstitial charge is more stable than the known *hP4* electride phase[24] from about 10 TPa to over 30 TPa. We have described the stability of the high-pressure electride phases in terms of the influence of the atomic cores on the valence electrons, Jones's Fermi-surface mechanism, the adoption of open structures to increase the occupied valence bandwidths, and interstitial electron blobs. The generality of these ideas and our results for Na, Mg and Al suggest that open structures should be very common in *sp*-bonded materials at terapascal pressures.

Methods

Density functional theory calculations. The density functional theory calculations were carried out with the CASTEP plane-wave code[26], ultrasoft pseudopotentials[27] and the Perdew–Burke–Ernzerhof generalized gradient approximation functional[28]. It is very important to use carefully constructed and tested pseudopotentials at multiterapascal pressures. We treated the 1*s* orbitals as core states whereas the other 11 electrons per atom were treated explicitly. The pseudopotential contained three non-local projectors for each of the *s* and *p* channels, and the *d* channel was taken as the local pseudopotential. We found a pseudopotential core radius of 1.4 a.u. to be sufficient to give small numerical errors in the enthalpy differences plotted in Fig. 1. For the searches we used a plane-wave basis-set cutoff of 500 eV and a Brillouin-zone integration grid of spacing $2\pi \times 0.07$ Å^{-1}. The structures were further relaxed at a higher level of accuracy consisting of a basis-set cutoff of 700 eV and a *k*-point grid spacing of $2\pi \times 0.05$ Å^{-1} to obtain the final results reported in this paper. The phonon calculations were carried out with a cutoff of 700 eV, a *k*-point grid spacing of $2\pi \times 0.07$ Å^{-1} and supercells containing 128 atoms (bcc) and 256 atoms (Al16–*I4/mcm*).

Strategy for structure searching. We started searching with two-atom unit cells at 1, 2 and 3 TPa, finding bcc to be the lowest-enthalpy structure. When we increased the pressure to 10 TPa we found the simple hexagonal structure to be the most stable. We then returned to lower pressures to find where non-close-packed structures first become stable. Various searches were carried out, the most extensive being at 5 TPa with cells containing 2, 4 and 8–21 atoms. Particularly low-enthalpy host–guest structures were found with 11, 16 and 21 atoms.

Received 7 December 2009; accepted 7 June 2010; published online 11 July 2010

References

1. Jeanloz, R. *et al.* Achieving high-density states through shock-wave loading of precompressed samples. *Proc. Natl Acad. Sci. USA* **104,** 9172–9177 (2007).
2. Hawreliak, J. *et al.* Modeling planetary interiors in laser based experiments using shockless compression. *Astrophys. Space Sci.* **307,** 285–289 (2007).
3. Batani, D. *et al.* Equation of state data for iron at pressures beyond 10 Mbar. *Phys. Rev. Lett.* **88,** 235502 (2002).
4. Lomonosov, I. V. Multi-phase equation of state of aluminum. *Laser Particle Beams* **25,** 567–584 (2007).
5. Vladimirov, A. S., Voloshin, N. P., Nogin, V. N., Petrovtsev, A. V. & Simonenko, V. A. Shock compressibility of aluminum. *Sov. Phys. JETP Lett.* **39,** 85–88 (1984).
6. https://lasers.llnl.gov/.
7. Akahama, Y., Nishimura, M., Kinoshita, K. & Kawamura, H. Evidence of a fcc–hcp transition in aluminum at multimegabar pressure. *Phys. Rev. Lett.* **96,** 045505 (2006).
8. Tambe, M. J., Bonini, N. & Marzari, N. Bulk aluminum at high pressure: A first-principles study. *Phys. Rev. B* **77,** 172102 (2008).
9. Pickard, C. J. & Needs, R. J. High pressure phases of silane. *Phys. Rev. Lett.* **97,** 045504 (2006).
10. Pickard, C. J. & Needs, R. J. Structure of phase III of hydrogen. *Nature Phys.* **3,** 473–476 (2007).
11. Pickard, C. J. & Needs, R. J. Highly compressed ammonia forms an ionic crystal. *Nature Mater.* **10,** 757–779 (2008).
12. Pickard, C. J. & Needs, R. J. Dense low-coordination phases of lithium. *Phys. Rev. Lett.* **102,** 146401 (2009).
13. Fortes, A. D., Suard, E., Lemé-Cailleau, M-H., Pickard, C. J. & Needs, R. J. Crystal structure of ammonia monohydrate II. *J. Am. Chem. Soc.* **131,** 13508–13515 (2009).
14. Nelmes, R. J., Allan, D. R., McMahon, M. I. & Belmonte, S. A. Self-hosting incommensurate structure of barium IV. *Phys. Rev. Lett.* **83,** 4081–4084 (1999).
15. McMahon, M. I. & Nelmes, R. J. High-pressure structures and phase transformations in elemental metals. *Chem. Soc. Rev.* **35,** 943–963 (2006).
16. Arapan, S., Mao, H-k. & Ahuja, R. Prediction of incommensurate crystal structure in Ca at high pressure. *Proc. Natl Acad. Sci. USA* **105,** 20627–20630 (2008).
17. Brazhkin, V. V. High-pressure synthesized materials: A chest of treasure and hints. *High Pressure Res.* **27,** 333–351 (2007).
18. Holian, K. S. A new equation of state for aluminum. *J. Appl. Phys.* **59,** 149–157 (1986).
19. Rousseau, B. & Ashcroft, N. W. Interstitial electronic localization. *Phys. Rev. Lett.* **101,** 046407 (2008).
20. Neaton, J. B. & Ashcroft, N. W. Pairing in dense lithium. *Nature* **400,** 141–144 (1999).
21. Jones, H. Applications of the Bloch theory to the study of alloys and of the properties of bismuth. *Proc. R. Soc. A* **147,** 396–417 (1934).
22. Ackland, G. J. & Macleod, I. R. Origin of the complex crystal structures of elements at intermediate pressure. *New J. Phys.* **6,** 138 (2004).
23. Von Schnering, H. G. & Nesper, R. How nature adapts chemical structures to curved surfaces. *Angew. Chem.* **26,** 1059–1080 (1987).
24. Ma, Y. M. *et al.* Transparent dense sodium. *Nature* **458,** 182–185 (2009).
25. Lundegaard, L. F. *et al.* Single-crystal studies of incommensurate Na to 1.5 Mbar. *Phys. Rev. B* **79,** 064105 (2009).
26. Clark, S. J. *et al.* First principles methods using CASTEP. *Z. Kristallogr.* **220,** 567–570 (2005).
27. Vanderbilt, D. Soft self-consistent pseudopotentials in a generalized eigenvalue formalism. *Phys. Rev. B* **41,** 7892–7895 (1990).
28. Perdew, J. P., Burke, K. & Ernzerhof, M. Generalized gradient approximation made simple. *Phys. Rev. Lett.* **77,** 3865–3868 (1996).

Acknowledgements

The authors were supported by the Engineering and Physical Sciences Research Council (EPSRC) of the UK.

Author contributions

C.J.P. and R.J.N. contributed extensively to all aspects of the work.

Additional information

The authors declare competing financial interests: details accompany the paper at www.nature.com/naturematerials. Supplementary information accompanies this paper on www.nature.com/naturematerials. Reprints and permissions information is available online at http://npg.nature.com/reprintsandpermissions. Correspondence and requests for materials should be addressed to C.J.P.

© 2010 Macmillan Publishers Limited. All rights reserved.